

Article

Capture and UV-Fluorescence Characterization of Primary Aerosols Ejected During the Fast Pyrolysis of Biomass in a Hot Plate Reactor

Mario A. Sánchez ^{1,*}, Estefanía Orrego-Restrepo ², Mariana Bustamante-Durango ¹, Juan C. Maya ², Farid Chejne ², Brennan Pecha ³ and Adriana M. Quinchía-Figueroa ¹

¹ Escuela de Ingeniería y Ciencias Básicas, Universidad EIA, Envigado 055428, Colombia; mabustamantedu@unal.edu.co (M.B.-D.)

² Grupo de Investigación TAYEA, Departamento de Procesos y Energía, Facultad de Minas, Universidad Nacional de Colombia-Sede Medellín, Medellín 050034, Colombia; eorregor@unal.edu.co (E.O.-R.); jcmaya@unal.edu.co (J.C.M.); fchejne@unal.edu.co (F.C.)

³ Renewable Resources and Enabling Sciences Center, National Renewable Energy Laboratory (NREL), Golden, CO 15013, USA

* Correspondence: mario.sanchez@eia.edu.co

Abstract: This study focuses on the collection and UV characterization of the bio-oil phase from primary aerosols ejected from the liquid intermediate phase during the fast pyrolysis of biomass in a hot plate reactor. The effects of the reactor pressure and aerosol-collecting surface temperature on the bio-oil yield and characteristics were evaluated. The study found that lower reactor pressures and a lower temperature of the collecting surface significantly enhanced the aerosol yield (up to 85%). UV-fluorescence was employed to assess the influence of these parameters on the light-to-heavy compound ratio (monomers vs. oligomers). The heavy fraction of bio-oil from the hot plate reactor was predominantly composed of dimers and trimers (340–370 nm), similar to pyrolytic lignin and the heavy fraction of the bio-oil, which also showed peaks in this range. In contrast, pyrolysis oils from auger and fluidized bed reactors displayed two peaks in the UV spectrum, with a maximum around 300 nm, indicating that they are mainly composed of light monomeric compounds. The UV characterization of the primary aerosols and the comparison with the UV spectra of the bio-oil and its fractions (light and heavy fraction and pyrolygnin) revealed similar UV prints, highlighting the importance of aerosol ejection in the final composition of bio-oil.

Keywords: bio-oil; aerosols; pyrolysis; biomass; UV-fluorescence; hot plate reactor



Citation: Sánchez, M.A.; Orrego-Restrepo, E.; Bustamante-Durango, M.; Maya, J.C.; Chejne, F.; Pecha, B.; Quinchía-Figueroa, A.M. Capture and UV-Fluorescence Characterization of Primary Aerosols Ejected During the Fast Pyrolysis of Biomass in a Hot Plate Reactor. *Reactions* **2024**, *5*, 1013–1026. <https://doi.org/10.3390/reactions5040053>

Academic Editors: Diogo M.F. Santos, Catarina Nobre, Paulo Brito, Margarida Gonçalves and Carmen Branca

Received: 30 August 2024

Revised: 2 November 2024

Accepted: 21 November 2024

Published: 1 December 2024



Copyright: © 2024 by the authors. Licensee MDPI, Basel, Switzerland. This article is an open access article distributed under the terms and conditions of the Creative Commons Attribution (CC BY) license (<https://creativecommons.org/licenses/by/4.0/>).

1. Introduction

1.1. Pyrolysis Oil Phases

Bio-oil derived from the fast pyrolysis of biomass is a complex blend of compounds formed from the breakdown of biomass pseudo-components, i.e., cellulose, hemicellulose, and lignin. Among the components of bio-oil are heavier elements such as lignin oligomers and various minerals. The presence of these heavier constituents in the bio-oil significantly impacts downstream processes, including hydrotreatment for fuel production.

Several studies have observed the formation of a liquid intermediate phase during biomass decomposition [1–5]. This liquid phase, called metaplast, consists of oligomeric products derived from cellulose, hemicellulose, and lignin. This phase not only affects transport phenomena within the particles and the residence time of intermediate products [6,7] but also, within this liquid phase, a bubbling phenomenon is seen and the subsequent collapse of these bubbles at the interface produces a liquid jet, which fragments into aerosol particles. These aerosols can transport non-volatile substances, contributing to the oligomeric and inorganic content of bio-oil [4,5,8,9].

The bio-oil fraction originating from aerosols ejected from the liquid intermediate phase during pyrolysis can constitute up to 20% wt. of the total oil yield [4]. This particular fraction is richer in lignin-derived components and anhydrosugars and contains lower levels of low-molecular-weight oxygenates from cellulose, such as hydroxyketones, compared to the overall collected oil [10].

1.2. Pyrolysis Oil UV Spectroscopy

UV spectroscopy or UV-visible spectrophotometry (UV-Vis or UV/Vis) is a simple, fast, and inexpensive method to determine the concentration of an analyte in a solution. The only requirement is that the sample absorbs in the UV-Vis region. In the UV-Vis technique, a beam with a wavelength varying between 170 nm and 850 nm passes through a solution in a cuvette. The wavelength region detected by a regular UV spectrometer is 200–380 nm for UV radiation, 380–750 nm for visible light, and above 750 nm for near-infrared radiation; the sample in the cuvette absorbs the UV and visible radiation [11,12]. In UV-fluorescence, the emitted radiant energy is measured, where compounds exhibiting fluorescence typically contain multiple fused aromatic rings or conjugated double bonds [13].

UV-fluorescence studies of pyrolysis bio-oils have revealed distinct emission peaks that correspond to different aromatic structures. Sun et al. [14] found that in rapeseed meal pyrolysis, a high-intensity fluorescence peak at 303 nm indicated structures containing 1–2 benzene rings, with additional peaks between 300 and 400 nm corresponding to dimers and trimers, and peaks beyond 400 nm indicating heavier oligomers. Manrique [15] similarly reported that pyrolytic lignin exhibited a small peak below 300 nm (monomers), two prominent peaks between 300 and 400 nm (dimers and trimers), and smaller peaks beyond 400 nm (heavier compounds). Consistent with this, Fonts et al. [13] identified emission peaks at 300 nm for phenols, 300–340 nm for oligomers, and above 340 nm for heavier lignin residues, demonstrating the ability of UV-fluorescence to differentiate phenolic monomers and oligomers based on their resonance and molecular size. Stankovikj et al. [16] investigated the quantification of functional groups in bio-oils from the pyrolysis of ten different biomass feedstocks, as well as in commercial bio-oils. The UV-fluorescence response demonstrated linearity within the 5 to 40 ppm range (diluted in methanol) for estimating lignin-derived mono- and oligophenols, with spectra showing three distinct peaks at 288, 328, and 354 nm.

The influence of the pyrolysis temperature on the bio-oil fluorescence and aromatic content was examined by multiple studies. Sun et al. [14] showed that under slow pyrolysis conditions, the fluorescence peak intensity reached a maximum at 500 °C and declined at higher temperatures due to increased cracking reactions. Zhang et al. [17] observed a fluorescence range of 270–350 nm at 400 °C, indicating compounds with 1–3 benzene rings, while higher temperatures of 600 °C favored heavier phenolic compounds. Similarly, Asadullah et al. [18] reported a peak in the bio-oil intensity at 550 °C, with subsequent thermal decomposition reducing aromatic concentrations at elevated temperatures. The findings emphasize that higher pyrolysis temperatures lead to the increased formation of heavier aromatic compounds, up to a thermal limit where decomposition prevails.

The further differentiation of aromatic structures in bio-oil was highlighted by various researchers. Du et al. [19] demonstrated that hydrodeoxygenation shifted the peak from below 290 nm (single-ring compounds) to 300–320 nm (two-ring compounds), with peaks above 320 nm representing multi-ring oligomers. Trubetskaya et al. [20] found bio-oil absorption bands near 280 nm ($\pi \rightarrow \pi^*$ transitions in aromatics) and around 325 nm (etherified hydroxyl groups), with heavier oligomers emitting near 343 nm. Additionally, Atashi et al. [21] observed that without a catalyst, light aromatics showed similar intensities at 320 nm, while the highest and lowest intensities of heavy aromatics at 360 nm were obtained using Ar and N₂ carrier gases, respectively. These studies illustrate that UV-fluorescence spectra effectively capture the molecular complexity and distribution of aromatic compounds in bio-oils.

1.3. Pyrolysis Oil Fractioning

Due to the significant polarity differences among bio-oil compounds, various separation strategies have been developed in recent years to separate the light and heavy phases of the bio-oil. One of the earliest methods reported involved solvent fractionation using water and diethyl ether, which proved to be effective in selectively fractionating compounds based on their molecular weights [22]. Later, they incorporated the use of dichloromethane into the scheme to separate the water-insoluble compounds, which produced a powder and a liquid phase, with high-molecular-mass lignin derivatives predominantly found in the powder phase [23]. Eventually, a refined solvent fractionation method was introduced, which incorporated centrifugation to accelerate the separation of water extracts [24].

Other similar methodologies for fractionation have been explored by various researchers. Ba et al. [25] conducted fractionation using cold water precipitation, yielding a precipitate of lignin derivatives. Their findings indicated that 29.6 wt% of the bio-oil was water-insoluble, 39.6 wt% consisted of water-soluble compounds, and 17.8 wt% comprised light compounds. Stankovikj et al. [26] analyzed the composition of the water-soluble fraction obtained through cold water precipitation from two commercial bio-oils (BTG[®] and Amaron[®]). They found that this fraction constituted 50.3 to 51.3 wt.% of the oils. In another study, Lian et al. [27] performed the extraction of bio-oil using ethyl acetate, obtaining an organic phase concentrated in phenols and an aqueous phase containing anhydrosugars. In turn, García-Pérez et al. [28] developed a scheme for characterizing bio-oils into chemical families, where before extraction with water and then diethyl ether or dichloromethane, they used toluene and methanol, followed by rotary evaporation and cold water precipitation.

In the present work, a novel experimental setup was used to capture primary aerosols through impact in a collecting surface in a hot plate reactor. The UV spectrum of the bio-oil obtained in the hot plate reactor was compared to the UV spectra of pyrolignin and UV spectra of the light and the heavy fractions of bio-oil obtained by condensation at different temperatures to shed light on the importance of the phenomenon of the thermal ejection of primary aerosols in the final composition of the bio-oil. The effect of process conditions like reactor pressure on the aerosol yield was also assessed.

2. Materials and Methods

2.1. Methodology for the Experimental Process

The methodology for the experimental process is divided into three sections; see Figure 1. In the first section, experiments using a hot plate reactor were performed to obtain bio-oil at different reactor pressures and aerosol-collecting surface temperatures.

In the second section, the UV spectrum for bio-oil from different feedstocks, as well as the UV spectra for bio-oil fractions and components (pyrolytic lignin) were obtained to compare these molecular prints to the UV spectrum of the collected bio-oil in the hot plate reactor. The light and heavy fractions of the bio-oil were obtained from the previous work of Uribe [29].

The third section corresponds to the analysis of the hot plate bio-oil samples using UV spectrometry to obtain information about the molecular print of the components within the bio-oil, including establishing the protocol and the analysis parameters to avoid redshift when performing the UV spectrometry. To analyze the molecular print of the bio-oil collected in the hot plate reactor, the UV spectrum of the collected sample was compared to the UV spectra obtained in the second phase [29].

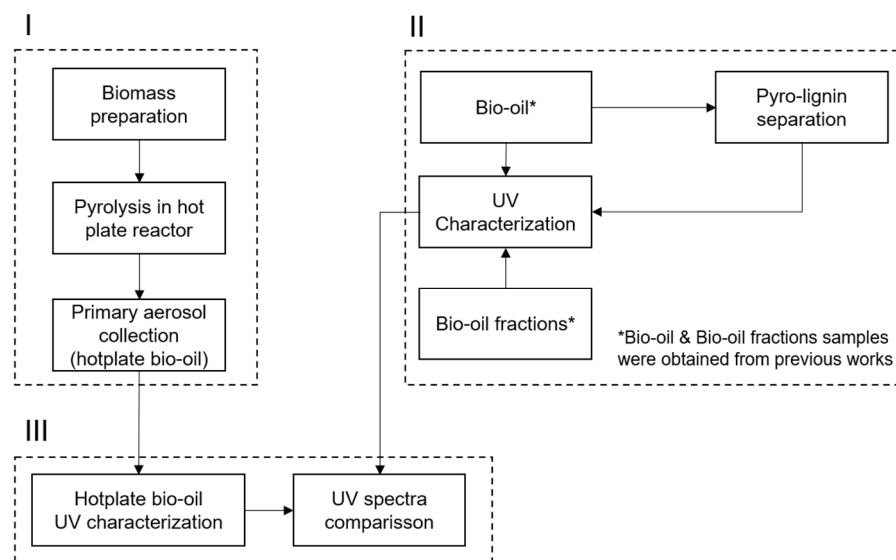


Figure 1. Schematic summary of the methodology (I, II, III correspond to the sections of the methodology).

2.2. Hot Plate Reactor

The hot plate reactor used in the present study allows one to pyrolyze biomass films between 30 and 300 μm with heating rates ranging from 10 to 1200 $^{\circ}\text{C}/\text{s}$. Parameters such as reactor pressure, inert gas of the reactor atmosphere, heating rate, reactor temperature, and holding time can be changed to study their effect on the product yield (char and total gases) and especially on the amount of collected bio-oil from aerosols. A scheme of the hot plate reactor is shown in Figure 2.

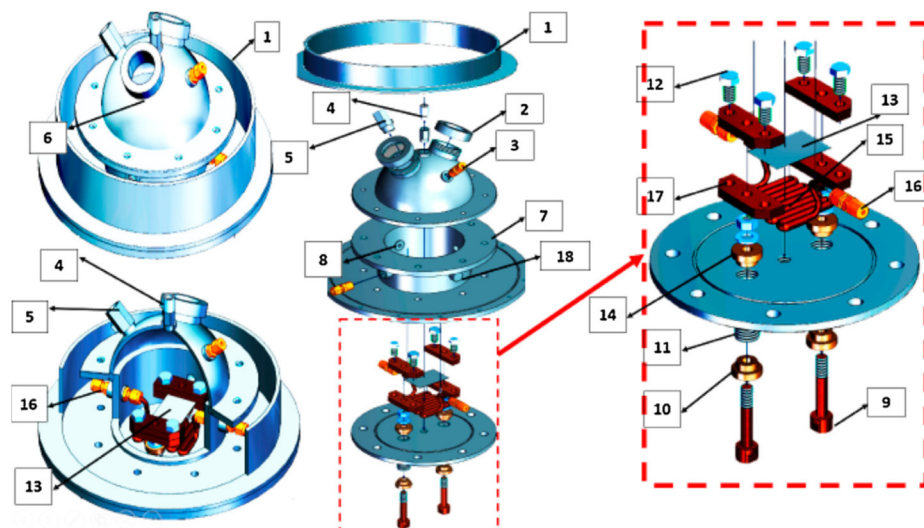


Figure 2. Hot plate reactor scheme: (1) Outer shell (for ice cooling). (2) Glass peephole. (3) Thermocouple port. (4) Pyrometer. (5) Port for gas sampling and vacuum pump connection. (6) Reactor top cover. (7) Reactor chamber. (8) Pressure sensor port. (9) Copper electrode. (10) Hermetic seal to isolate electric source. (11) Teflon insulation. (12) Electrode screws. (13) Steel plate for biomass heating. (14) Electrode screw adapter. (15) Cooling coil to refrigerate glass slide. (16) Port for CO_2/N_2 feeding. (17) Copper plates. (18) Purge gas port (components inside the dash red line correspond to the subassembly of the electric heating elements). Reproduced from [30], with permission.

The body of the hot plate reactor is constructed in 304 stainless steel sch 40. Two copper electrodes are connected to a steel plate of 6×4 mm with a thickness of 0.45 mm, where the biomass is impregnated for heating. A set of four aluminum plates (two at each

end) of 50×100 mm with 5 mm thickness are used as terminals to transfer the power to the steel plate where the biomass is heated. At the top of the reactor cover, a CT SF25 pyrometer with a spectral range of 8 to 14 μm connected to a PID control system, was used to measure the temperature of the biomass film which was impregnated in the steel plate. On the side of the reactor cover is installed a tap to plug a DRUCK-DPI 104 pressure sensor to measure the changes in reactor pressure; the accuracy of the sensor is 0.07 mbar. A type K thermocouple is located 30 mm above the steel plate to measure the temperature of the gas phase. A vacuum pump can be connected to a port, numbered as (5) in Figure 2; a Pfeiffer MVP006-4 pump (Pfeiffer Vacuum, Asslar, Germany) is used to reduce the pressure down to 150 mbar (abs.) during the pyrolysis experiments.

Under the steel plate, a cooling coil is installed to refrigerate a glass slide used for the collection of the aerosols. The glass slide is located on top of the cooling coil and below the steel plate. Cooling is used to avoid evaporation of the aerosols that impact the glass slide; a temperature of -10 $^{\circ}\text{C}$ is achieved by the expansion of a CO_2 flow inside the coil.

Port (16) in Figure 2 is used to provide the inert gas for the O_2 -free atmosphere for the pyrolysis process; N_2 or CO_2 can be used as the inert gas. The heating of the biomass film is achieved by supplying current from a 10 kW/220 V electric transformer. At nominal power, a heating rate of 1200 $^{\circ}\text{C}/\text{s}$ can be reached while the temperature recording is performed with a time delay of 10 ms with an accuracy of ± 6 $^{\circ}\text{C}$.

2.2.1. Biomass Sample Preparation

The biomass films to be impregnated in the steel plate are prepared by suspending finely ground sugarcane bagasse (Figure 3A) in distilled water. The suspension is prepared with a solid concentration of 10 wt.%. To impregnate the steel plate, a thin brush is dipped into the suspension of the biomass and used to paint over the central strip (60 mm long) (Figure 3B). The water from the suspension is then removed by slowly drying the sheet in a Mettler Toledo moisture balance (HB 34) under a halogen lamp at 80 $^{\circ}\text{C}$. The resulting dry film of biomass adhered to the plate surface is shown in Figure 3C. An average of $60 \mu\text{m} \pm 12 \mu\text{m}$ was used for the biomass film thickness based on the previous work by Montoya et al. [30].

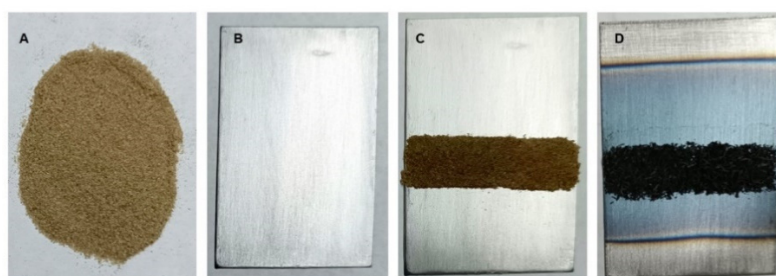


Figure 3. Preparation of film bagasse for the steel plate. (A) Raw ground biomass. (B) Steel plate. (C) Biomass impregnated on the steel plate. (D) Char layer after pyrolysis.

2.2.2. Hot Plate Reactor Experimental Design

The effect of two reactor parameters on product yields and bio-oil characteristics was studied; see Table 1. Two different reactor pressures were tested: a vacuum pressure of 0.150 bar and an atmospheric pressure (0.746 bar). Also, two temperatures for the aerosol-collecting surface were used: -10 $^{\circ}\text{C}$ and 20 $^{\circ}\text{C}$. Nitrogen was used as the inert gas for the pyrolysis, and the heating rate and final temperature of the biomass were constant at 100 $^{\circ}\text{C}/\text{s}$ and 500 $^{\circ}\text{C}$, respectively. No holding time was used during the experiments.

After the biomass was converted in the hot plate reactor, the steel plate was weighed to measure the char yield. Also, the bio-oil collected in the glass slide was weighed and then its UV-Vis spectrum (molecular print) was characterized using UV spectroscopy.

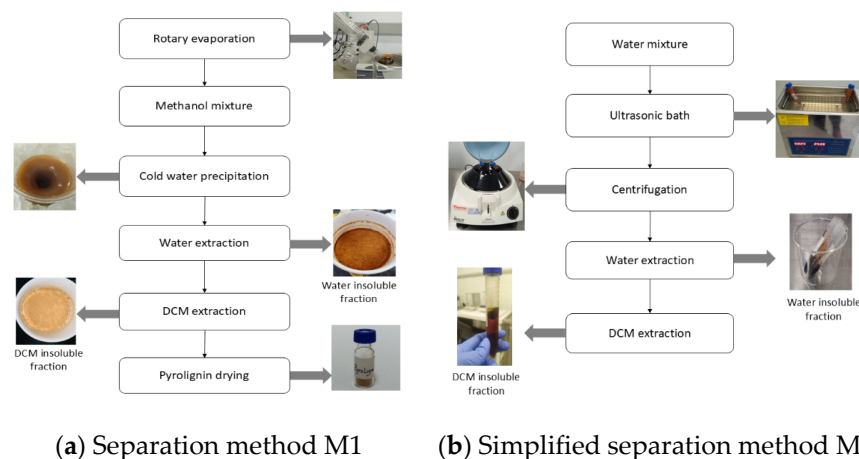
Table 1. Factors for experimental study.

| Factor | Levels | |
|--------------------------|------------------------|-----------|
| Biomass | Sugarcane bagasse | |
| Moisture content | Dry | |
| Mineral content | No washing | |
| Reactor atmosphere | N ₂ (99.9%) | |
| Heating rate | 100 °C/s | |
| Final temperature | 500 °C | |
| Reactor pressure (abs) | 0.150 bar | 0.746 bar |
| Collecting surface temp. | −10 °C | 20 °C |

2.3. Bio-Oil Fraction Separation

The comparison of the UV-spectrum of the collected sample with pyrolytic lignin is particularly important, as pyrolytic lignin is mainly composed of lignin-derived heavy components (oligomers). Its molecular print is expected to resemble that of the collected bio-oil, which mainly consists of primary aerosols composed of lignin oligomers directly ejected from the metaplast phase, which comes mostly from the lignin pseudo-component.

In the present work, two methods of obtaining the pyrolytic lignin were compared: a method involving rotary evaporation and cold water precipitation (M1) and a simplified method (M2). The first method was proposed by Manrique [15], where a rotary evaporator is employed to remove water from the bio-oil; then, the bio-oil is mixed with methanol in a concentration from 10 to 30%, and later, the lignin-derived components are separated from the sugars through cold water precipitation, as shown Figure 4. After cold water precipitation, the water-insoluble fraction, which is rich in lignin-derived components is mixed with dichloromethane (DCM) and the insoluble fraction is separated. This insoluble fraction corresponds to the pyrolytic lignin, which is rich in lignin oligomers.

**Figure 4.** Separation methods for pyrolytic lignin.

In the second method (M2) (see Figure 4), the bio-oil is mixed with water at a concentration of 10–30% with the aid of an ultrasonic bath. Then, the insoluble water fraction of the bio-oil is separated using a centrifugal machine at 10,000 rpm for 30 min. The obtained water-insoluble fraction is then mixed with dichloromethane and after manual mixing, a three-phase solution is obtained, where the insoluble fraction corresponds to the lignin-derived oligomers (pyrolytic lignin), based on the fraction method of Oasmaa et al. [24].

2.4. UV Spectroscopy Parameter Setup

As mentioned before, the objective of the present work was to evaluate the effect of some process parameters, like the reactor pressure and the temperature of the aerosol-collecting surface, on the molecular print (UV spectrum) of the collected bio-oil. A Duetta Horiba spectrophotometer (Horiba, Kyoto, Japan) was used for the UV spectrum measurements. These data were visualized and analyzed using EzSpec Software (Version 1.4.3.3) with Rayleigh masking correction. The synchronous spectra were normalized.

Redshift Phenomenon and Spectrophotometer Parameter Setup

During the UV spectroscopy of an analyte, the redshift phenomenon can be presented; this phenomenon occurs when there is a shift in the position of an emission band or peak of the analyte in the UV spectrum compared to its expected position in the absence of any perturbations. This shift can be caused by various factors, including changes in the electronic environment of the analyte, such as changes in the pH or solvent polarity, or by interactions with other molecules or ions present in the sample; these interactions can be affected by the concentration of the analyte [31,32].

In the present work, the bio-oil samples collected from the hot plate reactor were tested to evaluate the redshift phenomenon at concentrations ranging from 10,000 ppm to 4 ppm (concentration in methanol). For concentrations above 100 ppm, the redshift phenomenon has an important effect on the UV spectrum characterization; it was also found that for concentrations below 10 ppm, the emission intensity capture by the UV-fluorescence sensor was in the same range of the error, and for this reason, a concentration of 50 ppm was used for all the UV spectrum measurements. The final parameter setup for the UV spectrum measurements is presented in Table 2.

Table 2. Parameter setup for UV spectrum measurements.

| Parameter | Value | Units |
|---------------------------|----------|-------|
| Analyte concentration | 50 | ppm |
| Solvent | Methanol | - |
| Excitation range | 255–575 | nm |
| Excitation step increment | 2 | nm |
| Emission slip | 15 | nm |
| Emission range | 270–600 | nm |
| Excitation bandpass | 5 | nm |
| Emission bandpass | 10 | nm |
| Integration time | 0.2 | s |
| Detector accumulation | 5 | - |

3. Results

3.1. Characterization of Bio-Oil from Different Feedstocks

The bio-oils from different feedstocks produced in an auger reactor at 500 °C by Chávez et al. [33] as well as commercial BTG[®] oil were characterized by UV spectroscopy as a reference to compare the UV spectrum of the bio-oil obtained in the hot plate reactor [33].

Figure 5 shows that the UV spectrum for the different bio-oils shows a peak just below 300 nm, which corresponds to the light components (monomers), and two more peaks are seen around 340 nm and 370 nm, which correspond to heavier molecules (dimers and trimers), in accordance with the findings from previous studies by Sun et al. [14].

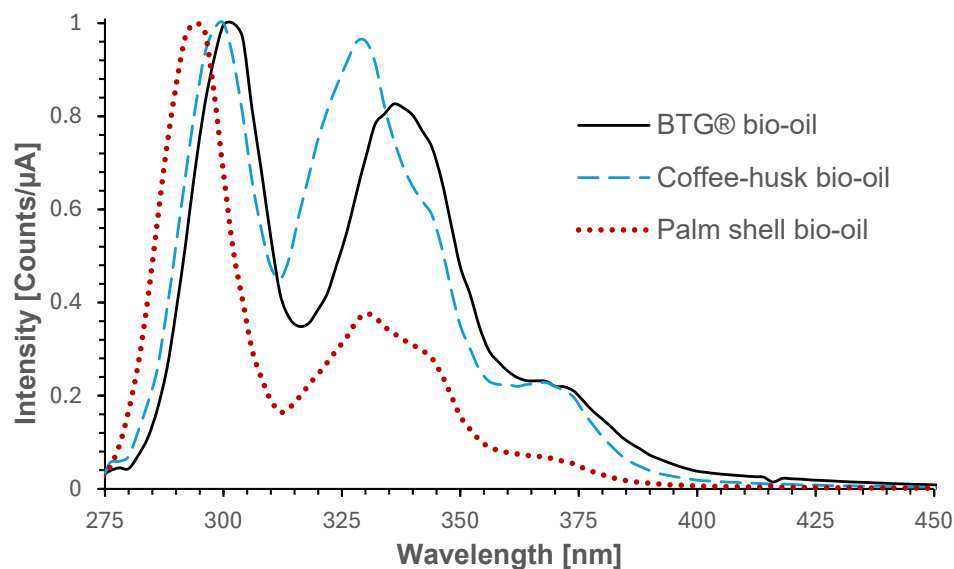


Figure 5. UV spectrum for bio-oils from different feedstocks: Commercial BTG[®], coffee-husk, and palm shell.

3.2. Characterization of Bio-Oil Fractions

The light and heavy fractions of the bio-oil obtained by Uribe [24] were characterized by UV spectrometry. Figure 6 shows the UV spectrum for both fractions. The heavy fraction exhibits three peaks: a first peak around 300 nm that corresponds to the monomeric compounds, a second peak around 340 nm corresponding to the oligomeric compounds (dimers and trimers), and a third peak (370 nm) corresponding to heavier oligomeric compounds. On the other hand, the lighter fraction of the bio-oil only exhibits one main peak around 300 nm which corresponds mainly to the monomeric compounds and dimers.

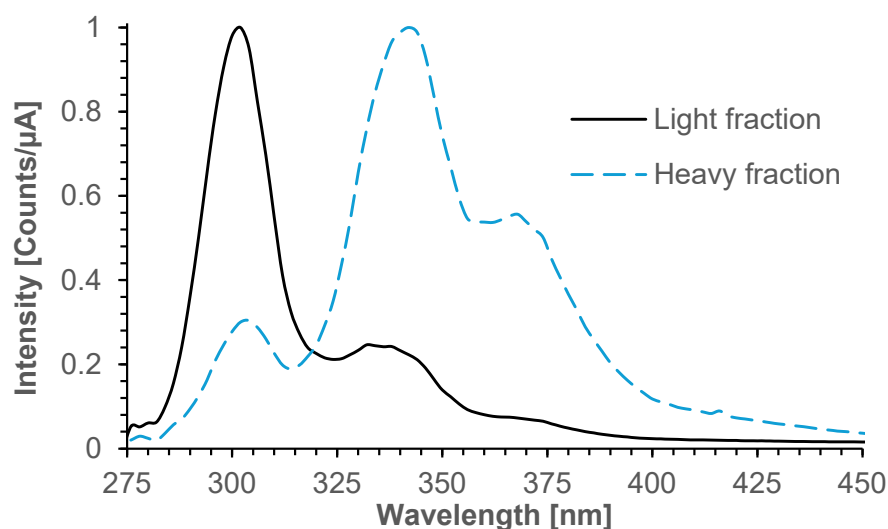


Figure 6. UV normalized spectra of the light and heavy fractions of pyrolysis bio-oil.

Regarding the 3D UV-fluorescence spectra, the heavier fraction exhibited a molecular print that was wider and more intense at higher wavelengths, indicating that this phase is richer in heavier compounds (dimers and trimers); see Figure 7.

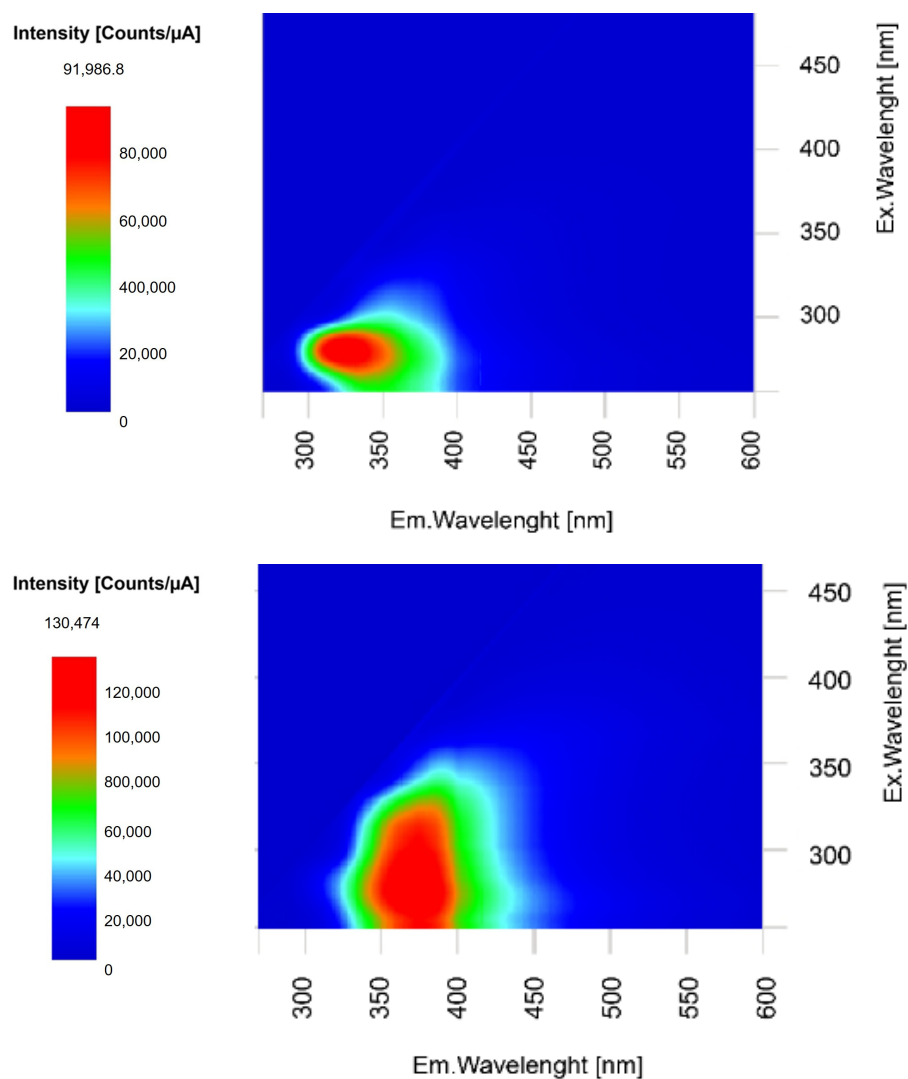


Figure 7. Three-dimensional UV-fluorescence spectra of the heavy and light fraction of pyrolysis bio-oil. Upper image: light fraction (mainly monomers). Lower image: heavy fraction (mainly oligomers).

3.3. Characterization of Pyrolytic Lignin

The UV spectra of the pyrolytic lignin obtained by both separation methods (M1 and M2) from BTG[®] oil are shown in Figure 8. Both spectra show a maximum peak around 340 nm, indicating that the mixture is mainly composed of dimers and trimers, in contrast with the UV spectrum of the commercial BTG[®] oil, which corresponds mainly to monomeric compounds. Also, Figure 8 shows a similar molecular print for the pyrolytic lignin obtained by both separation methods, indicating that the simplified method can separate with similar efficiency the sugars and monophenols from the lignin oligomeric compounds.

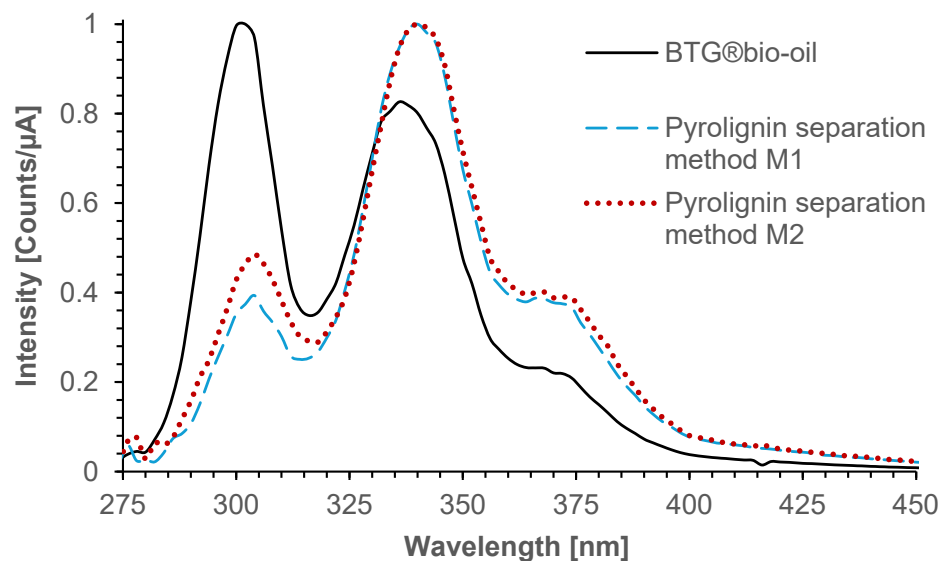


Figure 8. UV normalized spectra of the pyrolygnin obtained by the separation methods M1 and M2 and compared with the spectrum of commercial BTG® bio-oil.

3.4. Effect of Process Parameters on Bio-Oil Yield and Characteristics

The effect of the reactor pressure and the temperature of the aerosol-collecting surface on the yield of the bio-oil as well as the effect of these parameters on the UV spectrum (molecular print) were measured. Table 3 shows the effect of both parameters on the amount of bio-oil that was collected on the glass slide; since the glass slide does not capture the totality of the bio-oil produced in the hot plate, this yield corresponds to an apparent yield. For all the experiments, the biomass film was heated up to 500 °C, and a heating rate of ~100 °C/s was used.

Table 3. Effect of reactor parameters on bio-oil yields.

| Experiment | Pressure abs. (Bar) | Surface Temp. (°C) | Bio-Oil Yield (%) (Apparent) |
|------------|---------------------|--------------------|------------------------------|
| P1T1 | 0.746 (0 psig) | 20 | 14.8 ± 1.17 |
| P1T2 | 0.746 (0 psig) | −10 | 22.8 ± 0.9 |
| P2T1 | 0.150 (−10 psig) | 20 | 27.4 ± 2.2 |
| P2T2 | 0.150 (−10 psig) | −10 | 39.2 ± 2.6 |

Table 3 shows that the most predominant effect on the apparent yield of bio-oil corresponds to the pressure of the reactor, where a decrease in the pressure increases the amount of collected bio-oil, which can be explained due to an increase in the aerosol ejection phenomenon. An increase of 85% and 71% was found when the pressure of the reactor was decreased for temperatures of the collecting surface of 20 °C and −10 °C, respectively.

On the other hand, an effect of the collection surface temperature can also be observed: the apparent yield of bio-oil increased by 54% and 43% when the temperature of the collecting surface was reduced to −10 °C for manometric reactor pressures of 0.150 Bar(abs.) and 0.745 Bar(abs.), respectively. These results can be explained by an increase in the condensation of volatiles on the glass slide.

The previous hypothesis can be confirmed by the UV spectra of the bio-oil collected in the hot plate for the different conditions. Figure 9 shows that the bio-oil samples collected under vacuum conditions (P2T1 and P2T2) have a higher intensity of a peak around 375 nm, indicating a higher concentration of heavier compounds (dimers and trimers), which come from the aerosols ejected directly from the liquid intermediate phase (metaplast). Conversely, the bio-oil samples collected at lower temperatures of the collecting surface

show a higher intensity of the peak around 300 nm indicating a higher concentration of lighter compounds (monomers) due to the condensation of light volatiles on the top of the glass slide.

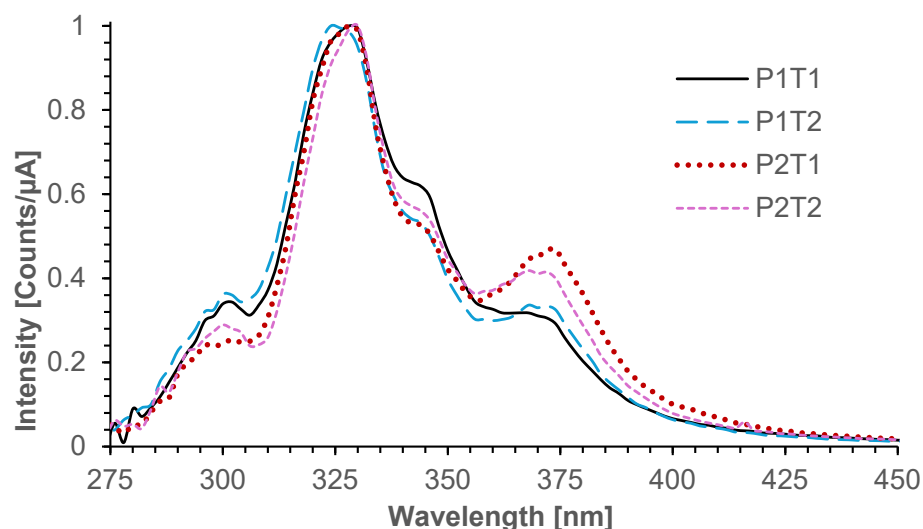


Figure 9. UV normalized spectra of the hot plate bio-oil at different conditions.

Despite the differences in the UV spectra between the bio-oil samples for the different reactor conditions, all the samples exhibit a similar UV spectrum with peaks at 325, 345, and 375 nm, corresponding to oligomeric compounds and a smaller peak at 300 nm corresponding mainly to monomeric compounds and light dimers. Figure 10 shows a comparison of the UV spectrum of a bio-oil sample collected from the hot plate reactor with the UV spectra from commercial BTG[®] pyrolysis oil and pyrolygnin. The UV spectrum of the hot plate bio-oil sample, similarly to the spectrum of the pyrolygnin, is composed mainly of heavier compounds (dimers and trimers), in contrast to the BTG oil, which is mainly composed of monomers, confirming that most of the bio-oil collected in the hot plate corresponds to aerosols that are ejected from the metaplast phase.

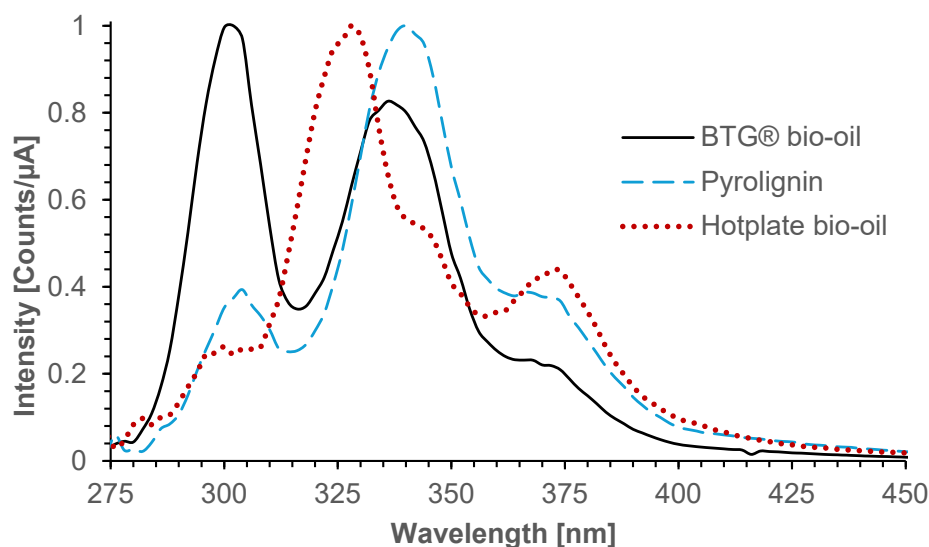


Figure 10. Comparison of the UV spectra of the commercial BTG[®] pyrolysis oil, pyrolygnin, and hot plate bio-oil.

4. Conclusions

The aerosol ejection phenomenon was found to be significantly influenced by process parameters such as the reactor pressure and the temperature of the collection surface for the aerosols. An increase in the bio-oil yield up to 85% was observed when the pressure of the reactor was reduced to 0.150 Bar(abs.) (−10 psig) and a temperature of −10 °C was used for the collecting surface. These results are important because, at larger scales, the conditions of the pyrolysis reactors could be optimized or reduce the amount of heavy lignin-derived components if an upgrading process, such as hydrotreatment, is used to separate the heavy fraction. Conversely, the process conditions can also be tailored to increase the final yield of these heavy oligomers if the bio-oil is intended for applications such as resin production.

In contrast to the bio-oil obtained in the hot plate reactor, the UV spectrum of the analyzed pyrolysis oil (BTG[®] pyrolysis oil, and coffee husk and palm oil from Auger reactor) showed that most of the bio-oil corresponds to monomers and other light compounds. The bio-oil collected in the hot plate reactor at different process conditions exhibited a similar molecular print (UV spectrum), with most of the bio-oil corresponding to oligomeric compounds (dimers and trimers) with main peaks at 325 nm, 345 nm, and 375 nm. The UV spectrum of the pyrolytic lignin shows that it is mainly composed of dimers and trimers, confirming that the collected aerosols in the hot plate reactor are ejected from the metaplast phase. Information about the primary aerosols and their UV spectra is important to analyze the extra-particle reactions of the aerosols as they travel through the reactor since the charring and cracking reactions will affect the final yield of the bio-oil fractions. Future work on aerosol extra-particle reactions can shed light on this phenomenon.

Despite the similar UV spectra, the effect of the process parameters on the molecular print of the hot plate bio-oil can also be observed, where the bio-oil samples collected at reduced pressures exhibited a higher concentration of heavier compounds, while the samples collected at lower temperatures exhibited a higher concentration of lighter compounds. These results can be explained by the higher intensity of the ejection phenomena at reduced reactor pressures and the higher condensation of volatiles on the bio-oil-collecting surface at lower surface temperatures.

Regarding the separation methods employed for the pyrolytic lignin extraction, both methods used during the experimental process can effectively separate lignin oligomers (pyrolytic lignin) from sugar-derived components and monophenols, allowing for a simple and fast method to extract pyrolytic lignin for characterization.

Author Contributions: Conceptualization, M.A.S., F.C., J.C.M., B.P., and A.M.Q.-F.; methodology, M.A.S., and E.O.-R.; validation, M.A.S., E.O.-R., and M.B.-D.; formal analysis, M.A.S., F.C., J.C.M., B.P., and M.B.-D.; investigation, M.A.S.; data curation, M.A.S., E.O.-R., and M.B.-D.; writing—original draft preparation, M.A.S., E.O.-R., and M.B.-D.; writing—review and editing, M.A.S., F.C., J.C.M., B.P., E.O.-R., and M.B.-D.; visualization, M.A.S. and M.B.-D.; supervision, M.A.S.; project administration, M.A.S.; funding acquisition, M.A.S. All authors have read and agreed to the published version of the manuscript.

Funding: This research was funded by EIA University, project “Modelado y evaluación experimental de la pirólisis rápida y autotérmica de biomasa”, code INVCO0452023.

Data Availability Statement: The data that support the findings of this study are available from the corresponding author, [M.A.S.], upon reasonable request.

Acknowledgments: The authors want to thank the Alliance for Biomass and Sustainability Research—ABISURE—Universidad Nacional de Colombia, Hermes code 53024, for its support in the realization of this study. The author Farid Chejne also wants to thank The Ministry of Science, Innovation, and Technology of the National Government for financing the project “Hybrid poly-generation scheme (Thermochemical-Biological) for the replacement of fossils from organic waste” (contract ICETEX 2022-0666) of the 890 call of the Ministry of Science, Innovation, and Technology of the National Government.

Conflicts of Interest: The authors declare no conflicts of interest. The funders had no role in the design of the study; in the collection, analyses, or interpretation of the data; in the writing of the manuscript; or in the decision to publish the results.

References

1. Lédé, J.; Blanchard, F.; Boutin, O. Radiant flash pyrolysis of cellulose pellets: Products and mechanisms involved in transient and steady state conditions. *Fuel* **2002**, *81*, 1269–1279. [[CrossRef](#)]
2. Boutin, O.; Ferrer, M.; Lédé, J. Flash pyrolysis of cellulose pellets submitted to a concentrated radiation: Experiments and modelling. *Chem. Eng. Sci.* **2002**, *57*, 15–25. [[CrossRef](#)]
3. Fisher, T.; Hajaligol, M.; Waymack, B.; Kellogg, D. Pyrolysis behavior and kinetics of biomass derived materials. *J. Anal. Appl. Pyrolysis* **2002**, *62*, 331–349. [[CrossRef](#)]
4. Montoya, J.; Pecha, B.; Janna, F.C.; Garcia-Perez, M. Micro-explosion of liquid intermediates during the fast pyrolysis of sucrose and organosolv lignin. *J. Anal. Appl. Pyrolysis* **2016**, *122*, 106–121. [[CrossRef](#)]
5. Zhou, S.; Garcia-Perez, M.; Pecha, B.; McDonald, A.G.; Westerhof, R.J.M. Effect of particle size on the composition of lignin derived oligomers obtained by fast pyrolysis of beech wood. *Fuel* **2014**, *125*, 15–19. [[CrossRef](#)]
6. Dufour, A.; Ouartassi, B.; Bounaceur, R.; Zoulalian, A. Modelling intra-particle phenomena of biomass pyrolysis. *Chem. Eng. Res. Des.* **2011**, *89*, 2136–2146. [[CrossRef](#)]
7. Pecha, B.; Arbelaez, J.I.M.; Garcia-Perez, M.; Chejne, F.; Ciesielski, P.N. Progress in understanding the four dominant intra-particle phenomena of lignocellulose pyrolysis: Chemical reactions, heat transfer, mass transfer, and phase change. *Green Chem.* **2019**, *21*, 2868–2898. [[CrossRef](#)]
8. Teixeira, A.R.; Mooney, K.G.; Kruger, J.S.; Williams, C.L.; Suszynski, W.J.; Schmidt, L.D.; Schmidt, D.P.; Dauenhauer, P.J. Aerosol generation by reactive boiling ejection of molten cellulose. *Energy Environ. Sci.* **2011**, *4*, 4306–4321. [[CrossRef](#)]
9. Jendoubi, N.; Broust, F.; Commandre, J.M.; Mauviel, G.; Sardin, M.; Lédé, J. Inorganics distribution in bio oils and char produced by biomass fast pyrolysis: The key role of aerosols. *J. Anal. Appl. Pyrolysis* **2011**, *92*, 59–67. [[CrossRef](#)]
10. Iisa, K.; Johansson, A.C.; Pettersson, E.; French, R.J.; Orton, K.A.; Wiinikka, H. Chemical and physical characterization of aerosols from fast pyrolysis of biomass. *J. Anal. Appl. Pyrolysis* **2019**, *142*, 104606. [[CrossRef](#)]
11. Skoog, D.A.; Holler, F.J.; Crouch, S.R. *Principles of Instrumental Analysis*; Cengage Learning: Boston, MA, USA, 2017.
12. Drago, R.S. *Physical Methods for Chemists*; Saunders College Pub.: Philadelphia, PA, USA, 1992.
13. Fonts, I.; Lázaro, C.; Cornejo, A.; Sánchez, J.L.; Afailal, Z.; Gil-Lalaguna, N.; Arauzo, J.M. Bio-oil Fractionation According to Polarity and Molecular Size: Characterization and Application as Antioxidants. *Energy Fuels* **2024**, *38*, 18688–18704. [[CrossRef](#)] [[PubMed](#)]
14. Sun, Y.; Li, C.; Zhang, S.; Dong, D.; Gholizadeh, M.; Wang, S.; Hu, X. Pyrolysis behaviors of rapeseed meal: Products distribution and properties. *Biomass Convers. Biorefin.* **2021**, *13*, 6575–6590. [[CrossRef](#)]
15. Manrique, R. Study of the Interaction Between the Heavy Fraction Oligomers from Pyrolysis Bio-Oil and the Catalyst in the Hydrotreatment Process. Ph.D. Thesis, Universidad Nacional de Colombia, Bogotá, Colombia, 2023.
16. Stankovikj, F.; McDonald, A.G.; Helms, G.L.; Garcia-Perez, M. Quantification of Bio-Oil Functional Groups and Evidences of the Presence of Pyrolytic Humins. *Energy Fuels* **2016**, *30*, 6505–6524. [[CrossRef](#)]
17. Zhang, Z.; Zhang, C.; Zhang, L.; Li, C.; Zhang, S.; Liu, Q.; Wang, Y.; Gholizadeh, M.; Hu, X. Pyrolysis of cellulose with co-feeding of formic or acetic acid. *Cellulose* **2020**, *27*, 4909–4929. [[CrossRef](#)]
18. Asadullah, M.; Ab Rasid, N.S.; Kadir, S.A.S.A.; Azdarpour, A. Production and detailed characterization of bio-oil from fast pyrolysis of palm kernel shell. *Biomass Bioenergy* **2013**, *59*, 316–324. [[CrossRef](#)]
19. Du, K.; Yu, B.; Xiong, Y.; Jiang, L.; Xu, J.; Wang, Y.; Su, S.; Hu, S.; Xiang, J. Hydrodeoxygenation of Bio-Oil over an Enhanced Interfacial Catalysis of Microemulsions Stabilized by Amphiphilic Solid Particles. *Catalysts* **2023**, *13*, 573. [[CrossRef](#)]
20. Trubetskaya, A.; von Berg, L.; Johnson, R.; Moore, S.; Leahy, J.; Han, Y.; Lange, H.; Anca-Couce, A. Production and characterization of bio-oil from fluidized bed pyrolysis of olive stones, pinewood, and torrefied feedstock. *J. Anal. Appl. Pyrolysis* **2023**, *169*, 105841. [[CrossRef](#)]
21. Atashi, F.; Gholizadeh, M.; Ataei, F. Pyrolysis analysis of polyethylene terephthalate: Effects of carrier gases (N₂, He, and Ar) and zeolite catalyst (A4) on yield. *J. Chem. Technol. Biotechnol.* **2022**, *97*, 3395–3405. [[CrossRef](#)]
22. Sipilä, K.; Kuoppala, E.; Fagernäs, L.; Oasmaa, A. Characterization of biomass-based flash pyrolysis oils. *Biomass Bioenergy* **1998**, *14*, 103–113. [[CrossRef](#)]
23. Oasmaa, A.; Kuoppala, E.; Solantausta, Y. Fast Pyrolysis of Forestry Residue. 2. Physicochemical Composition of Product Liquid. *Energy Fuels* **2003**, *17*, 433–443. [[CrossRef](#)]
24. Oasmaa, A.; Kuoppala, E. Solvent Fractionation Method with Brix for Rapid Characterization of Wood Fast Pyrolysis Liquids. *Energy Fuels* **2008**, *22*, 4245–4248. [[CrossRef](#)]
25. Ba, T.; Chaala, A.; Garcia-Perez, M.; Rodrigue, D.; Roy, C. Colloidal Properties of Bio-oils Obtained by Vacuum Pyrolysis of Softwood Bark. Characterization of water-soluble and water-insoluble fractions. *Energy Fuels* **2004**, *18*, 704–712. [[CrossRef](#)]
26. Stankovikj, F.; McDonald, A.G.; Helms, G.L.; Olarte, M.V.; Garcia-Perez, M. Characterization of the Water-Soluble Fraction of Woody Biomass Pyrolysis Oils. *Energy Fuels* **2017**, *31*, 1650–1664. [[CrossRef](#)]

27. Lian, J.; Chen, S.; Zhou, S.; Wang, Z.; O'Fallon, J.; Li, C.-Z.; Garcia-Perez, M. Separation, hydrolysis and fermentation of pyrolytic sugars to produce ethanol and lipids. *Bioresour. Technol.* **2010**, *101*, 9688–9699. [[CrossRef](#)]
28. Garcia-Perez, M.; Chaala, A.; Pakdel, H.; Kretschmer, D.; Roy, C. Characterization of bio-oils in chemical families. *Biomass Bioenergy* **2007**, *31*, 222–242. [[CrossRef](#)]
29. Uribe Vargas, C.A. Estudio de la Condesnación Fraccionada de los Gases de Pirólisis de Cisco de Café. Ph.D. Thesis, Universidad Nacional de Colombia, Bogotá, Colombia, 2022.
30. Montoya, J.; Pecha, B.; Roman, D.; Janna, F.C.; Garcia-Perez, M. Effect of temperature and heating rate on product distribution from the pyrolysis of sugarcane bagasse in a hot plate reactor. *J. Anal. Appl. Pyrolysis* **2017**, *123*, 347–363. [[CrossRef](#)]
31. Lakowicz, J.R. *Principles of Fluorescence Spectroscopy*; Springer: Boston, MA, USA, 2006. [[CrossRef](#)]
32. Valeur, B.; Berberan-Santos, M.N. *Molecular Fluorescence*; Wiley: Hoboken, NJ, USA, 2012. [[CrossRef](#)]
33. Chávez Tarazona, B.P. Evaluación de la Pirólisis Rápida en Reactor Tipo Auger (Doble Tornillo Sinfín) Para el Aprovechamiento de Biomásas Residuales de Origen Agroindustrial en el Departamento Norte de Santander. Ph.D. Thesis, Universidad Nacional de Colombia, Bogotá, Colombia, 2023.

Disclaimer/Publisher's Note: The statements, opinions and data contained in all publications are solely those of the individual author(s) and contributor(s) and not of MDPI and/or the editor(s). MDPI and/or the editor(s) disclaim responsibility for any injury to people or property resulting from any ideas, methods, instructions or products referred to in the content.